JOURNAL OF MATERIALS SCIENCE 33 (1998) 653–657

Reduction of interlayer Co^{2+} ions in fluorine mica using diethylene glycol

TOMOHIRO YAMAGUCHI*, KUNIO KITAJIMA
Department of Chemistry and Material Engineering, Faculty of Engineering, Shinshu University, Wakasato, Nagano 380, Japan

Reduction of interlayer Co^{2+} ions in expandable fluorine mica has been attempted. The polyol process using diethylene glycol as a reducing agent was employed. The Co^{2+}-exchanged mica was refluxed at about 225–235 °C in liquid diethylene glycol for 10–120 minutes. Consequently, zero-valence Co metal (Co^0) intercalated mica having a metallic grey colour was obtained by *in situ* reduction of interlayer Co^{2+} ions, showing different properties from Co^{2+}-exchanged mica as a precursor. The layer charge of Co-metal-intercalated mica is compensated by protons which are produced through the course of reduction of interlayer Co^{2+} ions. The reduced sample heated at 350 °C, which had no organic molecules, exhibited a basal spacing of 1.28 nm, indicating the presence of 0.34 nm cobalt metal clusters after subtracting the thickness of the host silicate layer. During the process of reduction in diethylene glycol, cobalt metal particles were expelled from the interlayers which grew to about 0.5 μm onto the external surfaces of host mica crystals with increasing refluxing time.

1. Introduction

Many studies on intercalation of inorganic polycations into the interlayer region of expandable clay minerals have been reported. The present authors have focused on expandable synthetic fluorine micas as host crystals for intercalation. These synthetic micas feature a large cation exchange capacity and high crystallinity. The variability of the layer charge also leads to the controlled pillar density and microporous properties for alumina [1–4] and chromia [5] pillared fluorine micas.

Recently, *in situ* reduction of interlayer cations such as Cu^{2+}, Ag^{+}, Pd^{2+} or Pt^{2+} in montmorillonite by a polyol process [6] using ethylene glycol has been reported [7–10]. In these cases, metal-intercalated phases similar to pillared clays are obtained. However, the reduction of the interlayer cations is usually accompanied by the precipitation of metal particles on the external crystal surfaces. These metal-supported montmorillonites are attracting attention with respect to their catalytic and microporous properties. Although this polyol process may also be extended to the preparation of metal-supported expandable clays with other metals, reduction of interlayer Co^{2+} ions by the polyol process has not been reported up to now. Therefore, we have attempted to reduce 3d transition-metal ions (Cu^{2+}, Ni^{2+} and Co^{2+}) into zero-valence metal (M^0) in the interlayers of cation-exchanged fluorine micas by the same procedure. Consequently, Cu^{2+} and Ni^{2+} ions in the interlayers of fluorine micas have been found to be reducible, while interlayer Co^{2+} ions are not reducible. We have then applied the polyol process of using glycerol to *in situ* reduction, instead of using ethylene glycol, and found that interlayer Co^{2+} ions in fluorine micas are reducible. However, the colour of the reduced product by glycerol was black.

The present work explores further the polyol process of using diethylene glycol (DEG), which has a boiling point between those of ethylene glycol and glycerol, for *in situ* reduction of interlayer Co^{2+} ions in expandable fluorine micas having higher layer charge. The aims of this paper are (i) to clarify whether interlayer Co^{2+} ions are reducible or not, (ii) to resolve the problem of charge compensation in the reduced products and (iii) to examine the effects of the larger host flakes and dense population of interlayer cations upon formation of the reduced products. In consequence, we have succeeded in reducing interlayer Co^{2+} ions, obtaining Co^0-metal-cluster-intercalated fluorine mica with a metallic grey colour.

2. Experimental procedure

The starting Na taeniolite having a layer charge of 0.8, $Na_{0.8}Mg_{2.2}Li_{0.8}Si_4O_{10}F_2$, was synthesized by the same procedure as described previously [11] and ground into powder of 44–75 μm by an agate mortar. It was then exchanged three times with a 0.1 mol dm^3 solution of $CoSO_4$ for 1 h at room temperature. The samples were washed with distilled water to remove

*To whom all correspondence should be addressed.

the excess salts. The Co^{2+}-exchanged micas were suspended in DEG and refluxed in an argon atmosphere at the reduction temperature for changing the colour of Co^{2+}–mica for 10–120 min to observe the effect of time on reduction. After reaction, the refluxed products were thoroughly washed with ethanol and dried in air at room temperature. A portion of the refluxed product was heated at the temperatures in the range 200–600 °C in Ar. The samples were then characterized by X-ray diffraction (XRD), scanning electron microscopy (SEM), ultraviolet (UV)–visible spectra, infrared (IR) spectra and N_2 adsorption measurements. For comparison, H^+-saturated fluorine mica (hereafter abbreviated to H^+–mica) was prepared by an acid (HCl) treatment at pH 1.5. H^+–mica was then heated and also characterized by XRD measurements. The refluxed product and Co^{2+}–mica heated at 350 °C in Ar, which are free from interlayer DEG or water molecules, were allowed to react with butylamine and heated again at 200 °C in air. The basal spacings of the products were then measured by XRD (Cu Kα) with preventing the samples from rehydration by water vapour in air. The refluxed product heated at 350 °C in Ar was also allowed to react with pyridine vapour, followed by the measurement of IR spectra.

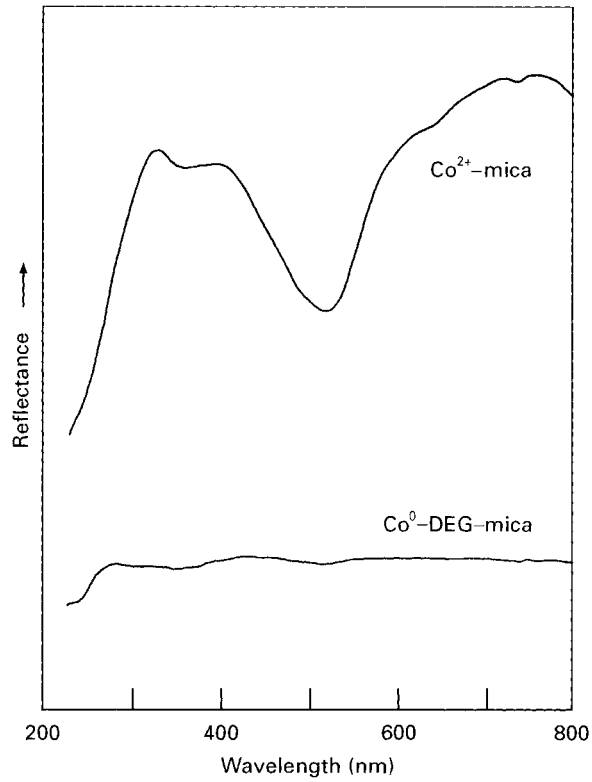

Figure 1 UV–visible spectra of Co^{2+}–mica and its refluxed product (Co^0–DEG–mica).

3. Results and discussion

3.1. Reduction of interlayer Co^{2+} ions

Fig. 1 shows UV–visible spectra of Co^{2+}–mica and its refluxed product in DEG for 90 min (hereafter abbreviated to Co^0–DEG–mica), obtained by a diffuse reflection method. The spectrum of Co^{2+}–mica is similar to that of the $[Co(H_2O)_6]^{2+}$ cation, giving an absorption band at 520 nm which results from the transition $^4T_{1g}(P) \leftarrow {}^4T_{1g}(F)$ [12, 13]. The colour of Co^{2+}–mica was pink. On the other hand, the spectrum of the refluxed product gives no absorption band corresponding to 520 nm, resulting in no sharp absorption bands in the visible region. The colour of the refluxed sample was metallic grey. It was also confirmed that refluxing of $Co(OH)_2$ in DEG in a similar manner results in the deposition of Co^0 metal and the UV–visible spectrum of these deposits resembles that of Co^0–DEG–mica. These results indicate that the reduction of $Co^{2+} \rightarrow Co^0$ in the interlayer region of Co^{2+}–mica occurs when Co^{2+}–mica is refluxed in DEG. The change in the colour of Co^{2+}–mica occurs at about 225–235 °C, indicating that the reduction of Co^{2+} takes place in this temperature range. When ethylene glycol is refluxed, the maximum temperature is up to 198 °C in ordinary atmospheric pressure, i.e., its boiling point; so it is not enough to reduce Co^{2+} ions to Co^0. On the other hand, when refluxed in glycerol at higher temperatures, Co^{2+}–mica changed its pink colour via a pale-purple colour into a dark-grey colour, probably owing to partial carbonization of intercalated glycerol molecules.

Powder XRD patterns of Co^0–DEG–mica and Co^{2+}–mica as a precursor are shown in Fig. 2. Co^{2+}–mica is a two-layer hydrated type, judging from

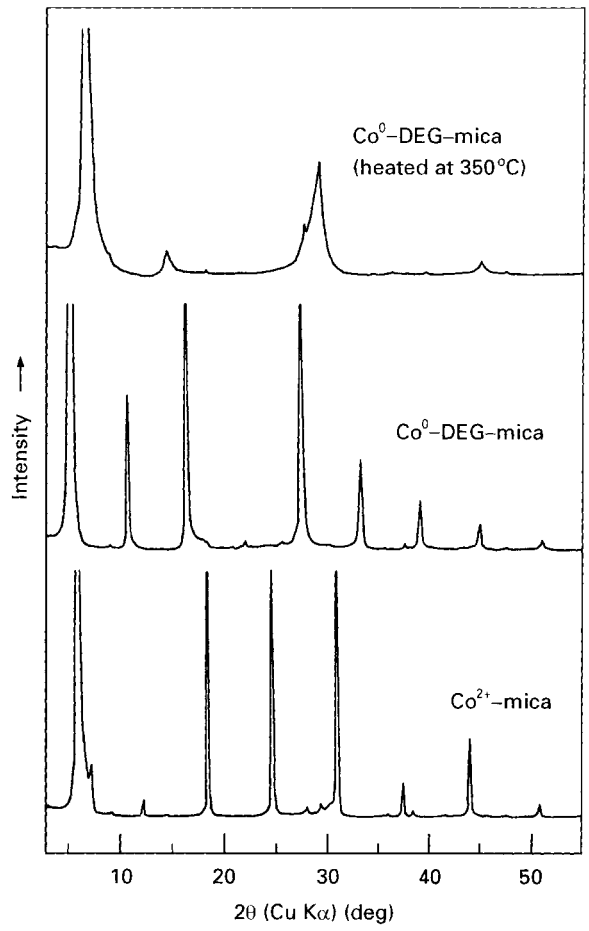

Figure 2 XRD patterns of Co^{2+}–mica, Co^0–DEG–mica and its thermally treated product at 350 °C.

the position of (0 0 1) diffraction. Co^0–DEG–mica gives the (0 0 1) peak at 5.4° (Cu Kα), showing the intercalation of DEG molecules of a double-layer type. According to Ravindranathan *et al.* [7] and Malla *et al.* [8, 9], the refluxed product of Cu^{2+}-exchanged montmorillonite in ethylene glycol has some copper metal particles deposited on external surfaces, as indicated by the diffraction peaks of Cu^0 metal particles. In our preliminary study of refluxing Cu^{2+}-exchanged mica in DEG or some other polyols, XRD patterns of the refluxed mica also showed the diffraction lines ascribable to Cu^0 metal particles. In contrast with these results for Co^{2+} reduction, XRD patterns of Co^0–DEG–mica and its heated product at 350 °C give no diffraction peaks attributable to Co^0 metal particles. The different behaviour of the metal precipitation in Cu^0–DEG–mica and in Co^0–DEG–mica reflects the difference in reducibility between Cu^{2+} and Co^{2+} cations. Thus, Cu^0 particles tend to be expelled onto the external surfaces, compared with Co^0 particles, owing to the reducibility of Cu^{2+}.

3.2. Charge compensation in reduced products

Fig. 3 shows IR spectra of pyridine adsorbed into Co^0–DEG–mica. The Co^0–DEG–mica was heated at 350 °C prior to exposure to pyridine vapour. There are no bands attributable to host mica crystals in this spectra. The absorption bands of 1440 and 1593 cm^{-1} are assigned to hydrogen-bonded pyridine molecules while those of 1485 and 1540 cm^{-1} are assigned to pyridinium cations [14]. The presence of pyridinium cations should indicate that Co^0–DEG–mica has proton acidity, suggesting that Co^0–DEG–mica has H^+ in the interlayer sites.

Fig. 4 shows the changes in XRD patterns of the samples treated with butylamine and then heated at 200 °C. Co^{2+}–mica and Co^0–DEG–mica heated at 350 °C, followed by the treatment with butylamine, give the (0 0 1) diffraction peaks at 6.4° and 6.1° (Cu Kα), respectively. This indicates the incorporation of

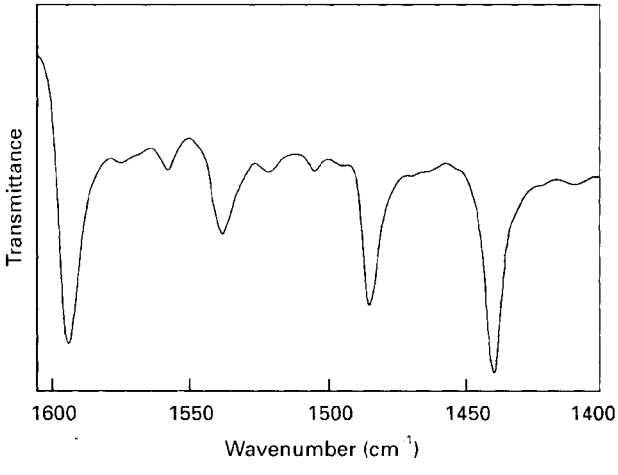

Figure 3 IR spectrum of Co^0–DEG–mica heated at 350 °C, followed by exposure to pyridine vapour.

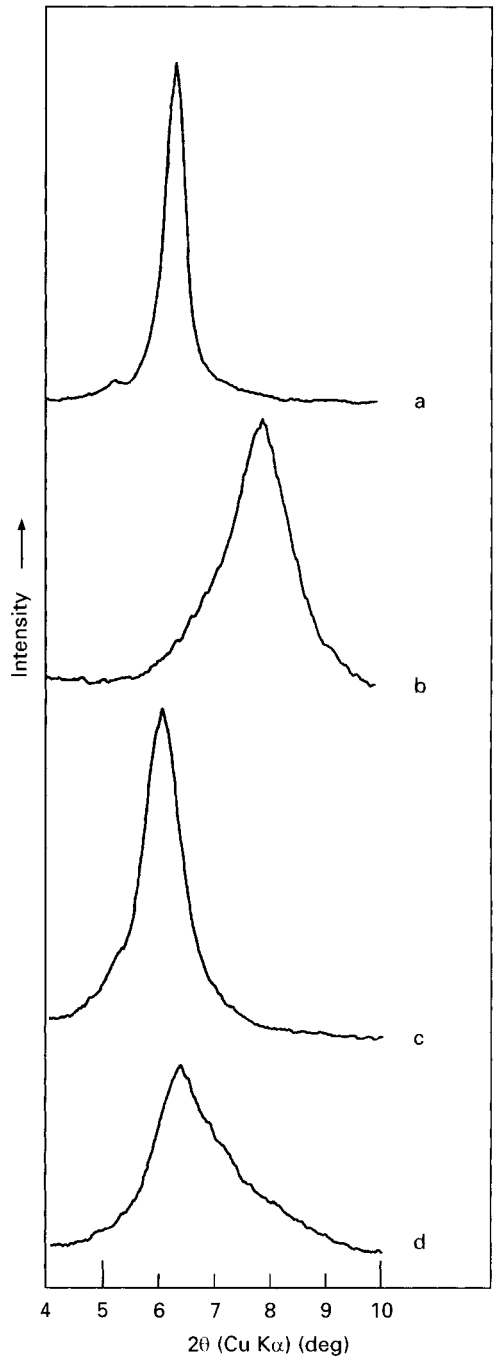

Figure 4 Changes in XRD patterns of micas treated with butylamine. Curve a, Co^{2+}–mica treated with butylamine; curve b, Co^{2+}–mica treated with butylamine and then heated at 200 °C; curve c, Co^0–DEG–mica treated with butylamine; curve d, Co^0–DEG–micas treated with butylamine and then heated at 200 °C.

butylamine molecules into the interlayer regions of fluorine micas. When heated at 200 °C, Co^{2+}–mica intercalated with butylamine gives the (0 0 1) diffraction peak at 7.9° (Cu Kα) while Co^0–DEG–mica intercalated with butylamine gives the (0 0 1) diffraction peak at 6.4° (Cu Kα). The difference between the thermal durabilities of butylamine-intercalated Co^{2+}–mica and Co^0–DEG–mica is due to the existence of H^+ in the interlayer regions of Co^0–DEG–mica. When Co^0–DEG–mica is intercalated with butylamine, the interlayer H^+ reacts with butylamine, forming a butylammonium ion. This process increases the thermal stability of the complex

because butylammonium ions are held by the Coulombic force, compensating the negative charge of silicate layers. On the other hand, in Co^{2+}–mica which has no H^+, the driving force of complexation is the interaction between Co^{2+} and the dipole moment of polar butylamine molecules. Therefore, the intercalated butylamine molecules are easily removed when heated at 200 °C.

These pyridine and butylamine tests substantiate the fact that Co^0–DEG–mica has H^+ in the interlayer regions. These interlayer protons are accompanied by the reduction of $Co^{2+} \rightarrow Co^0$ by DEG and compensate the negative layer charge of host mica crystals.

3.3. Basal spacing of reduced products

Fig. 5 shows the changes in basal spacings with increasing heating temperature for Co^0–DEG–mica and H^+–mica. Co^0–DEG–mica dried at room temperature gives a basal spacing of 1.64 nm. This indicates that the so-called α-type complex is formed, containing double layers of DEG molecules in the interlayer region. The basal spacing decreases stepwise with increasing heating temperature. The first decrease in the lower temperature region is due to the removal of organic molecules from the interlayer of the complex. The basal spacing of Co^0–DEG–mica heated at 350 °C is about 1.28 nm. However, the basal spacing further decreases to reach the constant value of 1.03 nm when heated above 500 °C. On the other hand, H^+–mica dried at room temperature gives a basal spacing of 1.47 nm. This indicates that double layers of water molecules exist in the interlayer region. Dehydration of H^+–mica occurs upon heating and the basal spacings of H^+–mica heated above 200 °C give the constant value of about 1.03 nm. Moreover, Co^{2+}–mica gave a basal spacing of 0.95 nm after calcination above 600 °C. In these respects, thermal behaviour of Co^0–DEG–mica is different from those of H^+–mica and Co^{2+}–mica. The difference between the basal spacings of Co^0–DEG–mica and H^+–mica in the temperature range from 200 to 350 °C is about 2.5–3.0 nm. In addition, the IR absorption bands ascribable to organic molecules were not observed for Co^0–DEG–mica heated above 300 °C. These results indicate that the basal spacing of Co^0–DEG–mica should reflect the size of Co^0 metal clusters encapsulated in the interlayer region of host crystals, although charge compensation in Co^0–DEG–mica crystals is due to protons as described before. In other words, the intercalated Co^0 metal clusters should determine the basal spacing of Co^0–DEG–mica, propping the silicate sheets apart as pillars at least in the temperature range from 300 to 350 °C.

Thus, the dimension of intercalated Co^0 clusters perpendicular to the silicate layer is estimated to be about 0.34 nm, which is calculated by subtracting the thickness of the silicate layer (0.94 nm) from the basal spacing at 350 °C. This relatively small clearance space seems to result from the high layer charge of host crystals, which gives strong interlayer bonding. Judging from the clearance space and atomic radius, the intercalated Co^0 clusters have only two or three atoms in that direction. The dimension of intercalated Co^0 clusters parallel to the silicate layer has not been known so far. Microporous characteristics were not observed by N_2 absorption because of its small clearance space.

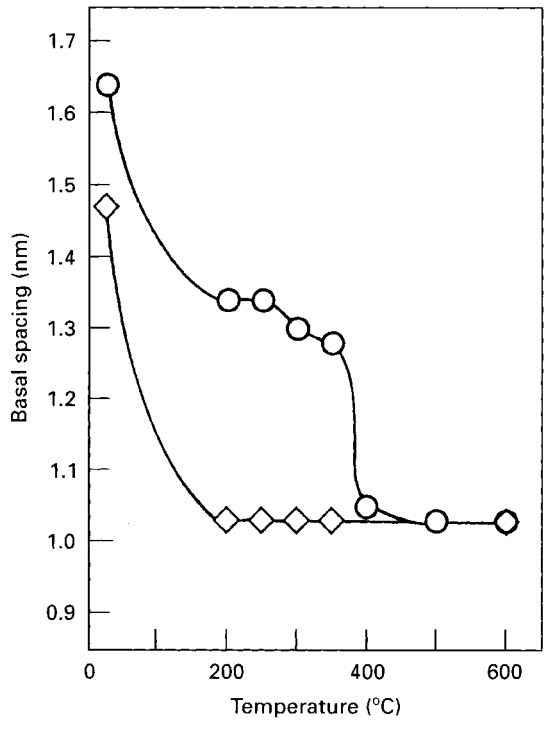

Figure 5 Basal spacings of Co^0–DEG–mica (○) and H^+–mica (◇) plotted against heating temperature.

3.4. Precipitation of Co^0 metal particles on external surfaces of host crystals

Although XRD recordings of Co^0–DEG–mica give no peaks of Co^0 metal particles, a slight amount of Co^0 metal particles deposited on external surfaces of host crystals has been found by SEM observation.

Fig. 6 shows SEM photographs of Co^0–DEG–mica which were prepared by refluxing for 10, 30 and 90 min, followed by heating at 350 °C. Spherical particles deposit on external layer-structured surfaces of mica crystals refluxed for 30 and 90 min, as shown in Fig. 6b and c. These particles were identified as Co^0 metal by energy-dispersive X-ray microanalysis. The sizes of deposited particles are less than 0.5 μm. On the other hand, Co^0 metal particles are undetectable in the product refluxed for 10 min, as seen in Fig. 6a. The amount of precipitated Co^0 particles increased with prolongation of the refluxing time at its initial stage. The loss of positive charge during $Co^{2+} \rightarrow Co^0$ reduction results in the expulsion of Co^0 clusters onto the outer surfaces, followed by the crystal growth which precipitates as fine metal particles. In the initial stage of reduction, the deposition of Co^0 metal particles occurs on the crystal edges along the cleavage lines, i.e., on the "cliffs" of host crystals, and not on the cleavage planes as seen in Fig. 6b. This means that the

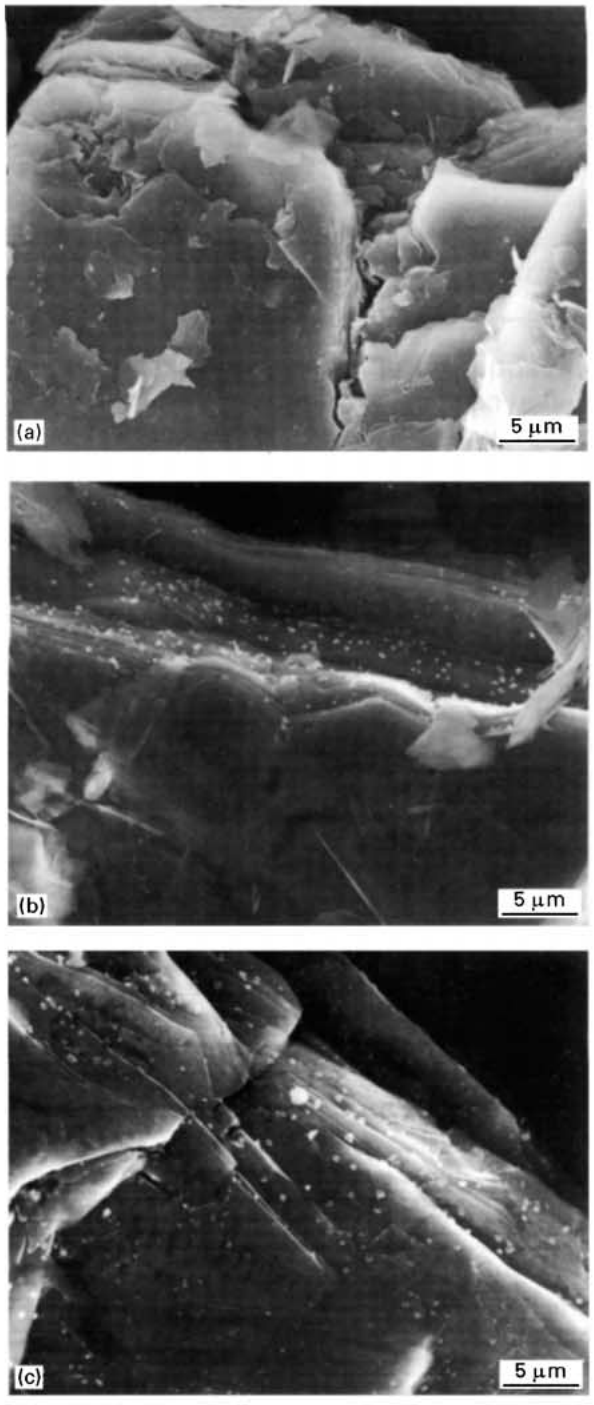

Figure 6 SEM photographs of Co^0–DEG–mica prepared by refluxing for 10–90 minutes: (a) refluxed for 10 min; (b) refluxed for 30 min; (c) refluxed for 90 min. The Co^0–DEG–mica were heated at 350 °C before SEM observation.

precipitation of Co^0 particles results from two-dimensional diffusion of Co^0 atoms or clusters along the interlayer regions. Since the larger flakes of mica crystals have a longer diffusion path for Co^0 atoms or clusters and migrate along the *a*, *b* crystal directions, the rate of M^0 precipitation for larger mica flakes should be slower than for finer montmorillonite flakes. This enables a larger amount of Co^0 clusters to be enclosed in the interlayer regions, at least in the early stage of $Co^{2+} \rightarrow Co^0$ reduction, compared with the case for montmorillonite. In addition to the size effects of host crystals, larger amounts of Co^0 clusters derived from the dense population of interlayer Co^{2+} ions are very likely to lengthen the lifetime of Co^0-metal-intercalated mica. Although a charge transfer mechanism through the interaction of metal cluster with surface oxygens [8, 9] may be effective for stabilization of metal clusters in the interlayers, prolongation of refluxing time leads to an increase in the amount of Co^0 metal particles on the external surfaces of fluorine mica crystals, yielding Co^0 metal clusters supported in and on mica.

4. Conclusions

We have tried to synthesize fluorine micas intercalated with 3d transition-metal clusters via corresponding ion-exchanged micas using various polyols. In this paper, we have investigated the preparation of Co^0-metal-intercalated fluorine mica using DEG as a reducing agent, and the results are summarized as follows.

1. The interlayer Co^{2+} ions in expandable fluorine mica are reducible by refluxing in DEG about 225–235 °C.

2. In Co^0-metal-intercalated fluorine mica, the interlayer protons accompanied by the reduction $Co^{2+} \rightarrow Co^0$ compensate the negative layer charge of host crystals.

3. Although some Co^0 metal particles are expelled onto the external surfaces of host crystals with prolongation of refluxing time, the Co^0 metal clusters enclosed in the interlayer region should prop the silicate layer apart, yielding Co^0-metal-cluster-intercalated mica.

References

1. T. FUJITA, K. KITAJIMA, S. TARUTA and N. TAKUSAGAWA, *Nippon Kagaku Kaishi* (1993) 1123.
2. *Idem., ibid.* (1993) 1312.
3. *Idem., ibid.*, (1994) 538.
4. T. YAMAGUCHI, T. FUJITA, N. TAKUSAGAWA and K. KITAJIMA, *ibid.* (1996) 307.
5. T. FUJITA, S. MATSUKURA, T. YAMAGUCHI, N. TAKUSAGAWA and K. KITAJIMA, *ibid.* (1995) 277.
6. F. FIEVERT, J. P. LAGIER, B. BLIN, B. BEAUDOIN and M. FIGLARZ, *Solid State Ionics* **32–33** (1989) 198.
7. P. RAVINDRANATHAN, P. B. MALLA, S. KOMARNENI and R. ROY, *Catal. Lett.* **6** (1990) 401.
8. P. B. MALLA, P. RAVINDRANATHAN, S. KOMARNENI and R. ROY, *Nature* **351** (1991) 555.
9. P. B. MALLA, P. RAVINDRANATHAN, S. KOMARNENI, E. BREVAL and R. ROY, *J. Mater. Chem.* **2** (1992) 559.
10. S. KOMARNENI, M. Z. HUSSEIN, C. LIU, E. BREVEL and P. B. MALLA, *Eur. J. Solid State Inorg. Chem.* **32** (1995) 837.
11. K. KITAJIMA, F. KOYAMA and N. TAKUSAGAWA, *Bull. Chem. Soc. Jpn.* **58** (1985) 1325.
12. Y. TANABE and S. SUGANO, *J. Phys. Soc. Jpn.* **9** (1954) 753.
13. A. B. P. LEVER, "Inorganic electronic spectroscopy" (Elsevier, Amsterdam, 1968) p. 112.
14. E. P. PARRY, *J. Catal.*, **2** (1963) 371.

Received 24 February
and accepted 19 August 1997